Catalysis Letters 9 (1991) 261–272

COORDINATION, ATOM REORGANIZATION, AND CATALYSIS OF PALLADIUM IN ZEOLITE CAGES

Wolfgang M.H. SACHTLER, Fernando A.P. CAVALCANTI and Zongchao ZHANG

V.N. Ipatieff Laboratory, Center for Catalysis and Surface Science, Northwestern University, Evanston, IL 60208, U.S.A.

Zeolite encaged palladium clusters undergo thorough atomic reorganizations when exposed to an adsorptive such as carbon monoxide or when used as catalysts e.g. in CO hydrogenation. Exposure to carbon monoxide of metal particles, which are initially anchored to zeolite walls via proton bridges, transforms the metal clusters into small, highly mobile carbonyl clusters. They coalesce and form larger clusters. At low temperature, this process is limited by the geometric constraints of the cage windows. At higher temperatures, further growth of metal particles occurs, conceivably via partial destruction of the zeolite matrix. The interaction of the metal particles with zeolite protons gives rise to electrondeficient metal clusters, which catalyze neopentane at a much higher rate than neutral metal particles. Such clusters might also act as collapsed bifunctional sites in bifunctional catalysis.

Keywords: Palladium cluster in zeolite cages, metal restructuring in zeolites, electron deficient metal clusters

1. Introduction

Chemisorption on metal surfaces is a complicated phenomenon. Chemical bonds are formed between atoms of the adsorbate and metal atoms. If chemisorption is dissociative, bonds between atoms of the adsorptive are broken. In 1962, we showed that the heat of adsorption in general also includes endothermic terms due to the partial rupture of metal-metal bonds [1,2]. From observations of the changes in surface topography due to chemisorption of nitrogen or carbon monoxide on the surface of a tungsten single crystal in a field ion microscope we concluded, in 1966, that strong chemisorption on transition metals is, in general, accompanied by a *reconstruction* of the metal surface [3–10]. At low temperatures this reconstruction is first observable at "open" crystal faces; the more close packed faces are "corroded" from their edges with the former faces. We called this reconstruction phenomenon "corrosive chemisorption" in analogy to Roginsky's earlier observation of "catalytic corrosion" on working Pt catalysts in the oxidation of ammonia to nitric oxide.

Surface reconstruction as a phenomenon, inherent in strong chemisorption, was further observed on evaporated metal films, where it leads to a time and

temperature dependent change of the electronic work function. In the 1960's and 1970's, it became clear that the reconstruction process is of particular relevance to alloy surfaces, where it leads to chemisorption induced segregation of one alloy component to the surface [11–15].

It was found that a given alloy particle easily adjusts its surface structure to the nature of the chemisorbing molecules. If the composition of the gas phase is changed, the composition of the adsorbing surface readjusts itself. Surface reconstruction is, therefore, of rather fundamental importance for the understanding of thermodynamics and kinetics of chemisorption and heterogeneous catalysis. Unfortunately, the importance of this phenomenon was often underestimated in the period when surface science workers concentrated their interest on macroscopic single crystal faces of high atomic density and negligible edges to more open faces; for such specimen surface reconstruction is, indeed, minimal. For technical catalysts, however, consisting of small metal particles on supports of high surface area, the mobility of exposed metal atoms will be high for each particle. It is intuitively expected that these atoms will easily rearrange upon chemisorption to acquire the configuration representing minimum free energy of the metal/adsorbate system. Little is known, however, of the actual reconstruction of such small particles.

For the study of chemisorption on very small metal particles, zeolite supports offer optimum conditions, because the dimensions of zeolite cages and channels impose strong sterical restrictions on the mobility of the metal particles. At low temperature, the particles larger than cage windows are prevented from coalescing with each other; fairly uniform metal particles can thus be prepared, permitting a "*catalyst-by-design*" strategy. Ligated metal clusters, e.g. carbonyls or hydrido-carbonyls, which otherwise tend to rapidly interact with each other, can also be thoroughly studied when they are isolated in a zeolite cage of appropriate size, as was found for rhenium hydrido carbonyls [16]. On the other hand, ligated clusters larger than the cage windows can be formed from smaller primary particles by a process called the "*ship-in-a-bottle*" technique [17–20].

In the present paper, we shall first summarize our present understanding of the elementary processes which determine the genesis of zeolite metal particles and thus permit control of their size. Palladium will be chosen as the example for a zeolite supported metal, with a fairly well understood mechanism of particle genesis. We shall then review recent results on the interaction of carbon monoxide with very small Pd particles – single atoms, tetrahedra and octahedra – inside the cages of zeolites, to illustrate chemisorption induced mobility, agglomeration and redispersion of metal particles. This will be followed by a brief review on the catalysis of CO hydrogenation with zeolite supported mono- and bifunctional catalysts. Finally, the formation of palladium-proton-adducts and their functioning as "*electron-deficient*" metal sites and as "*collapsed bifunctional sites*" will be mentioned.

Much of the research is still in progress and some conclusions are preliminary.

Other data have been published or submitted for publication; in this case, short summaries of the conclusions will be given, together with references to more detailed papers.

2. Genesis of palladium particles in zeolite Y

Zeolite Y of faujasite structure was used in this work. The major structural features of this zeolite are the large pore and window diameters of the three-dimensionally interconnected supercages. Additional features are the sodalite cages and hexagonal prisms of high negative charge density. The locations of Pd ions after various pretreatment conditions have been clearly identified by several techniques, including UV-VIS diffuse reflectance and EXAFS spectroscopy [21], temperature programmed oxidation (TPO) and reduction (TPR) [22], and X-ray diffraction [23–25]. After ion exchange, divalent palladium tetraammine ions are located in the supercages. They remain stable at calcination temperature (T_c) of 150 °C, as evidenced by their absorption peak at 33.5 kK, which is the characteristic absorption maximum of $Pd(NH_3)_4^{2+}$ ions. At $T_c = 250$ °C, cis-$Pd(NH_3)_2^{2+}$ ions prevail in the supercages [26]. After reduction of these ions at 200 °C, Pd_4 tetrahedra are formed in supercages [27], but the metal dispersion drastically decreases with increasing reduction temperature (T_R) [28]. Calcination of the same precursors above 300 °C results in complete oxidation of ammine ligands and concommitant migration of naked Pd^{2+} ions to sodalite cages. At $T_c = 500$ °C, some fraction of the Pd^{2+} ions is located in the hexagonal prisms, as evidenced by the increased backscattering of Al and Si in the second nearest neighbor EXAFS signal of Pd^{2+} [21]. After mild reduction, isolated Pd atoms have been found in the sodalite cages; interestingly, they are unable to dissociatively chemisorb dihydrogen [23–25,27,29]. At higher reduction temperatures, the Pd atoms migrate and coalesce in supercages [27,29]. At $T_R = 350$ °C, the average Pd particle size corresponds to octahedral Pd_6 [30]. The dispersion $D = F(T_R)$ curve for samples calcined at $T_c = 500$ °C has a maximum at 350 °C [29]. The strong interaction of reduced Pd primary particles with zeolite protons, which are a coproduct of the reduction process, has been found to be instrumental for the stabilization of the extremely small Pd particles [31]. This point will be further discussed in the next section. The presence of Pd ions can dramatically enhance the reducibility of other transition metal ions inside the same zeolite, provided that the latter ions are located in the proximity of the palladium [32–34].

3. Carbon monoxide induced agglomeration of Pd clusters

Extensive reorganization of Pd atoms has been identified upon adsorption of CO at room temperature. Exposing Pd/NaY that was reduced at low tempera-

ture to carbon monoxide at low pressure leads to spontaneous formation of a novel Pd cluster carbonyl, which is detected by its highly structured FTIR spectrum and is supposed to contain a core of 13 Pd atoms [18,20]. This nuclearity was, indeed, verified by EXAFS [27,30]. The $Pd_{13}(CO)_x$ cluster interacts with zeolitic protons, resulting in an electron-deficient hydridocarbonyl cluster [19,31]. Smaller bare Pd clusters that are anchored to the cage walls by protons become mobile when chemisorbing CO; the chemisorption bond appears to weaken the $Pd-H^+$ bond. The release of protons is evidenced by a significant increase of the FTIR intensity of the band due to hydroxyl groups after CO admission. This indicates that the primary Pd metal particles after reduction were, indeed, anchored to the cage wall via strong proton bridges [27,31]. Astonishing results were found with samples in which the primary Pd particles were either isolated atoms in small cages or Pd_4 or Pd_6 clusters in supercages. When such samples were exposed to CO at room temperature, EXAFS showed that the particle nuclearity changed spontaneously: in all cases a new carbonyl cluster is immediately formed with an average Pd coordination number of six, corresponding to $Pd_{13}(CO)_x$ clusters. This process is irreversible: upon removing CO, the Pd_{13} clusters do not disintegrate. This shows that formation of the $Pd_{13}(CO)_x$ clusters is determined by kinetic, rather than thermodynamic causes. Its mechanism has been rationalized by considering the migration and coalescence of primary Pd carbonyl clusters [27]. It appears that a primary carbonyl cluster can shed some of its CO ligands when passing through a cage window; the mobility of the primary Pd carbonyl clusters and their chance to grow by coalescence thus depends critically on the size of the metal core with respect to the diameter of the cage windows. This growth stops at room temperature when the critical composition of $Pd_{13}(CO)_x$ has been reached, because the Pd_{13} core has a diameter of 8.2 Å, but the window between the adjacent supercage is only 7.5 Å wide. At higher temperature, the zeolite lattice is no longer rigid and larger particles can be formed. The mechanistic model thus explains why our FTIR spectra recorded at room temperature show the signature of the $Pd_{13}(CO)_x$ clusters, irrespective of the preceding calcination program.

The conclusion that the dimension of the supercage windows dictates the core size in the final Pd carbonyl cluster has been confirmed recently by applying the above technique to Pd in a different zeolite, viz. the molecular sieve 5A. The supercages have similar dimensions in zeolites 5A and Y, but the window diameter between adjacent supercages is much smaller in 5A: 5 Å instead of 7.5 Å. It was found by EXAFS that the same treatment which produced $Pd_{13}(CO)_x$ clusters in zeolite Y, leads to $Pd_6(CO)_y$ clusters in zeolite 5A [35]. The value of y depends on the CO partial pressure; the molar ratio CO/Pd ranges from 0 to 1.6 in the p_{CO} range of 0 to 760 Torr.

The FTIR spectrum of $Pd_6(CO)_4$ differs strikingly from that of $Pd_{13}(CO)_x$. Whereas the latter spectrum shows doubly and triply bridged CO absorption in addition to terminal CO, the IR spectrum of the $Pd_6(CO)_yH^+$ cluster displays

only terminal and triply bridged CO. These IR spectral features of the $Pd_6(CO)_yH^+$ in zeolite 5A remarkably resemble those of the known carbonyl clusters $Rh_6(CO)_{16}$ or $Ir_6(CO)_{16}$, except that the triply bridged CO band in $Pd_6(CO)_yH^+$ is more intense than the terminal CO band, while the intensity ratio is reversed for $Rh_6(CO)_{16}$ or $Ir_6(CO)_{16}$.

The observation that, at 760 Torr of CO pressure and 21° C a green-colored palladium carbonyl is formed in 5A, is of importance in view of the common practice to determine metal dispersion in supported catalysts by CO adsorption. The observed CO_{ads}/Pd ratio is near 1.2 at 300 Torr and increases to 1.6 at 500 Torr of CO suggesting that the metal cores reconstruct again; conceivably a mononuclear tetracarbonyl $Pd(CO)_4$ starts to be formed at high CO pressure i.e. a homolog of the well known $Ni(CO)_4$.

At the time of writing this text, this research is still in progress. A conclusion which can be safely drawn is, however, that the surface reconstruction, which was reported in 1966 for CO adsorption on metal crystals, is even more intense for small metal particles in zeolites, where chemisorption induced metal atom reorganization is not only confined to the surface atoms of the adsorbing particle, but can also include migration and coalescence of particles.

4. CO hydrogenation on Pd/zeolite catalysts

The production of CH_3OH by CO hydrogenation over Pd catalysts was first reported in 1979 [37]. Since then, numerous studies have been published which were concerned with fundamental issues of this reaction. Structure sensitivity, promotion, and the electronic state and chemisorptive properties of Pd particles have been addressed by several groups [38–41]. The results and conclusions summarized in the previous sections of this paper provide a promising base for exploring some unresolved issues concerning CO hydrogenation on zeolite supported Pd catalysts.

We addressed the question concerning the structure sensitivity of this reaction by using catalysts consisting of well-defined Pd_{13} clusters or larger Pd particles supported on NaY and prepared according to the methods discussed in section 2. It was found that selectivity and time-on-stream behavior of Pd/NaY catalysts is strongly dependent on the initial size of the Pd clusters [42].

Catalysts that after reduction contain highly dispersed Pd particles ($H/Pd^0 \approx 0.7$) initially show a high activity and almost 100% selectivity towards CH_4. Activity and selectivity decrease sharply during the first few hours of reaction. During this period, CH_3OH and CH_3OCH_3 (DME) carbon yields increase by a factor of at least ten. As the production of these products passes through a maximum, the formation of higher hydrocarbons (C_{2+}) starts and rapidly increases. These hydrocarbons are highly branched and saturated, with a maximum

selectivity for the C_4 fraction. No aromatics have been detected. After about 8 hours of reaction, the carbon yields reach their final order: $C_{2+} > CH_4 > CH_3OH > DME$. This selectivity, as well as the catalyst activity, remain practically unchanged after an additional 12 hours of reaction.

In contrast, catalysts that have a low metal dispersion ($H/Pd^0 = \approx 0.1$) after reduction show an entirely different behavior. High carbon yields of CH_3OH and DME are observed from the start of the reaction, while the CH_4 carbon yield decreases only slightly. After a period of about 4 hours, the catalyst activity reaches a maximum which remains nearly constant for another 16 hours. The carbon yields also reach their final values during this initial period, this being $DME > CH_3OH \approx CH_4 \gg C_{2+}$. The small amount of C_{2+} hydrocarbons formed consists mostly of ethane and propane, the rest being mostly linear hydrocarbons.

The state of the Pd metal on these catalysts, before and after reaction, has been characterized by EXAFS, XPS and FTIR of adsorbed CO. They indicate unequivocally the presence of large Pd particles after reaction, independently of the initial dispersion of these catalysts. This is consistent with CO-induced Pd agglomeration. For the conditions discussed in section 3, i.e. room temperature and no reacting gas present besides CO, this agglomeration was limited by the geometric requirement that the core of a migrating carbonyl cluster must be able to pass through the cage window. For the more severe conditions of CO hydrogenation, with temperatures above 200 °C and H_2O vapor as a major product, this limitation is no longer valid. Particles that are much larger than the window of a rigid zeolite matrix can migrate and coalesce, conceivably by

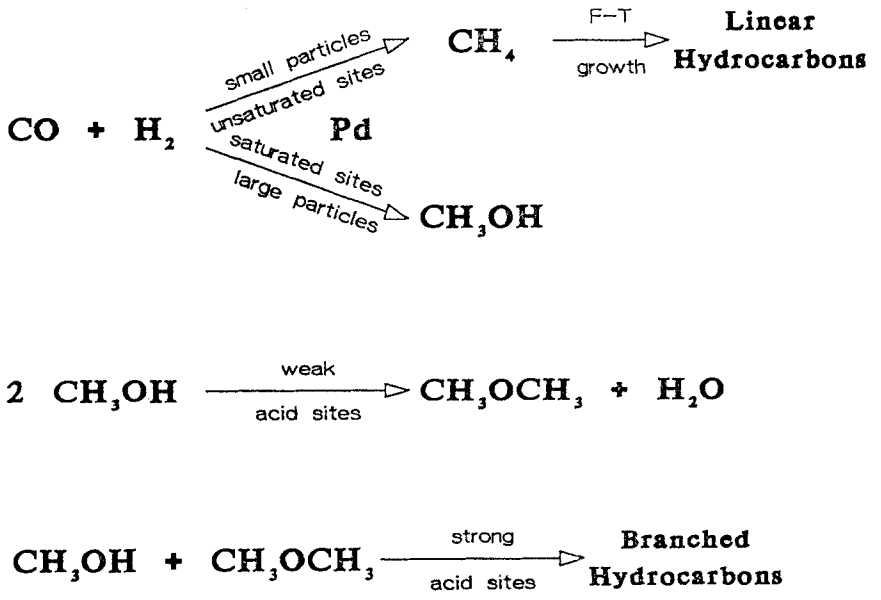

Fig. 1. Reaction scheme of CO hydrogenation over small and large Pd particles on an acidic support.

destroying part of the zeolite matrix. Moreover Ostwald ripening, i.e. detachment of metal atoms from one particle and their attachment on another particle, might occur. Previously we had observed that the decrease of metal dispersion with reduction temperature consists of two processes with different activation energy [28]. They might, likewise, be identified as passage through intact windows and higher activation energy processes such as Ostwald ripening or local zeolite collapse, respectively.

The present reaction and characterization studies offer strong evidence, in our interpretation, for the conclusion that CO hydrogenation over Pd/NaY catalysts is strongly structure sensitive. This is schematically summarized in fig. 1.

Several other issues concerning this reaction are still under study. They include the effect of the charge balancing cations on catalyst activity and selectivity, the effect of the number and strength of the acid sites on C_{2+} hydrocarbon formation. Zeolites of different structures will be compared; the exact location of the Pd particles and the structural integrity of the zeolite matrix after reaction have to be verified. At this stage, it is clear that the interaction of CO with Pd particles under reaction conditions is much more complex than previous studies, e.g. those involving macroscopic single crystals, were able to demonstrate.

5. Zeolite supported Pd-proton adducts

Protons are formed as a coproduct of the reduction of metal ions with hydrogen. The majority of these protons will be attached to oxygen ions of the cage walls, where they are identified by their characteristic O–H vibration bands in the IR spectrum or by their strong Brønsted acidity, which is manifest in the adsorption of Lewis bases and in heterogeneous catalysis. More recently it was found, however, that part of the protons created during metal ion reduction, can remain attached to metal atoms or metal particles. In the case of palladium, complexes of the type $[Pd_nH_z]^{z+}$ are formed. In this entity, the positive charge is not localized on the nucleus of the hydrogen atom, but will be distributed over the hydrogen and palladium atoms. The palladium thus becomes "*electron-deficient*". It is conceivable that the proton acquires a position intermediate between the cage wall and the Pd_n particle. In this model, the electron-deficient particle will be anchored to the cage wall via a hydrogen bridge. Evidence for this has been mentioned above: when small Pd particles chemisorb CO and coalesce to larger particles, the *intensity of the OH band increases*.

IR spectra of adsorbed CO permit discrimination between neutral and positively charged Pd atoms. An IR band at 2120 cm^{-1} of adsorbed CO on a mildly reduced Pd/NaY was ascribed by Sheu et al. [19] to CO adsorbed on a $[Pd–H]^+$ entity in a sodalite cage. The attachment of the CO molecule to this species will then take place through the O_6 ring between supercage and sodalite cage. A similar observation was reported by Tri et al. [43] for Pt/NaHY. These authors

found the stretching frequency of adsorbed CO shifted from 2090 cm^{-1} to 2068 cm^{-1} when the Pt/NaHY sample was neutralized with NaOH.

Electron-deficient Pd or Pt in zeolites is, however, not limited to isolated metal atoms. There is substantial physical evidence for the existence of electron deficient multiatomic particles of these elements in faujasite supercages. XPS data of Foger and Anderson [44] show a shift in binding energy for platinum in Pt/NaY and Pt/LaY. While these data are debatable in view of the masking of the XPS signal of Pt by the Al signal, recent data of Stakheev in our lab with Pd/HY show unambiguously that the binding energy of Pd is shifted towards higher values with respect to the same samples after neutralization of the protons [45]. Likewise, the Auger parameter of Pd in Pd/HY shows values in between those of neutral Pd and positive Pd ions.

The shift in the IR frequency of adsorbed CO was studied in detail for a variety of samples by Zhang et al. [31]. It was found that the intensity of the blue shifted IR band increases not only with the concentration of protons in the zeolite, but it could even be correlated with the local concentration of protons inside the supercages carrying Pd particles. It is of interest that an IR frequency shift in the opposite direction has been reported by Bezoukhanova et al. [46] for adsorbed CO and NO on Pt in basic zeolites. The authors conclude that, in these systems, the Pt particles carry a negative charge.

There is considerable chemical and catalytic evidence for the existence of electron-deficient metals in acidic zeolites. Dalla Betta and Boudart [47] found that the hydrogenolysis rate of neopentane is 40 times larger on 1 nm Pt aggregates in Y zeolites than on Pt supported on conventional supports. Likewise, it was found for Pd/NaHY that the catalytic activity per exposed and accessible Pd atom for this reaction was almost two orders of magnitude higher than that of Pd/SiO_2 catalysts tested in the same apparatus under the same conditions [48]. Neopentane conversion, in contrast to most other hydrocarbon conversions, does not cause catalyst deactivation because the neopentane molecule is not able to form olefins or carbenium ions [49]. This makes the reaction exceptionally appropriate for determining the intrinsic activity of metal/zeolite catalysts. In other catalytic work Gallezot et al. [29] showed that the high resistance of Pt/NaY to sulphur is due to electron deficiency. They correlated empirical parameters such as the ratio of the adsorption coefficients of benzene and toluene to electron deficiency. They observed that the thus defined extent of electron deficiency increases with the acidity of the zeolite.

Evidence for the formation of $[Pd_n - H_z]^{z+}$ adducts inside zeolites has also resulted in a novel heuristic model for bifunctional catalysis. A case in point is the ring enlargement of methylcyclopentane to cyclohexane. There is convincing evidence that the decisive rearrangement of the carbon skeleton takes place in a transition state which can be described as similar to a carbenium ion, consisting of the original five-membered ring and a protonated three-membered ring fused to it [50]. The classical model for reactions catalyzed by bifunctional catalysts

assumes shuttling of reaction intermediates between sites: the methylcyclopentane molecule is dehydrogenated on a metal site; the unsaturated product migrates to an acidic site, where the skeletal isomerization takes place; an olefinic product, e.g. cyclohexene, is released from the acid site and is hydrogenated when contacting, again, a metal site.

It has been suggested that on a palladium-proton adduct no shuttling is required, all reaction steps can be carried out during one residence of the adsorbed molecule on the same adduct [51]. The adduct thus functions as a "*collapsed bifunctional site*". Evidence supporting this model has been obtained by comparison of the rate of ring enlargement of methylcyclopentane under identical conditions on two catalysts: (1) Pd/HY, (2) a physical mixture of HY and Pd/NaY where all protons formed during reduction of the metal were subsequently neutralized by reaction with sodium azide. Both catalysts exposed the same number of metal and acid sites, but the Pd/HY sample had an initial ring enlargement activity roughly 40 times higher than the physical mixture. This result shows the importance of close proximity of metal sites and protons inside the same zeolite; it suggests that proton-palladium adducts are present in Pd/HY and that these act as "collapsed bifunctional sites" [50]. Subsequent temperature programmed surface reactions studies further revealed a substantial difference in catalytic performance between neutral Pd sites and Pd-proton adducts, the latter sites not only promote ring enlargement as mentioned, but are much less active in ring opening than neutral Pd sites [52].

In summarizing this section, it appears that the physical and chemical evidence lends credence to the model of palladium-proton adducts which act both as electron-deficient metal sites and as collapsed bifunctional sites in heterogeneous catalysis.

Acknowledgements

The authors gratefully acknowledge support from the Department of Energy, contract DE-FG02-87ER13654, for research on multimetal/zeolite systems, and from the National Science Foundation, contract CTS-8911184, for research on Pd particles and Pd carbonyl clusters in NaY.

References

[1] W.N.H. Sachtler and L.L. van Reijen, J. Res. Inst. Catalysis Hokkaido Univ. 10 (1962) 87.
[2] W.M.H. Sachtler and L.L. van Reijen, Shokubai 4 (1962) 147.
[3] A.A. Holscher and W.M.H. Sachtler, Disc. Faraday Soc. 41 (1966) 29.
[4] W.M.H. Sachtler, Angewandte Chemie 80 (1968) 155.
[5] W.M.H. Sachtler, Angewandte Chemie 80, (1968) 673.

[6] W.M.H. Sachtler, Angewandte Chemie, International Edition 7 (1968) 668.
[7] A.A. Holscher and W.M.H. Sachtler, in: *Molecular Processes at Solid Surfaces*, ed. E. Drauglis (McGraw-Hill, New York, 1969) p. 317.
[8] R. Bouwman, H.P. van Keulen and W.N.H. Sachtler, Ber. Bunsenges. f. phys. Chem. 74 (1970) 198.
[9] B.E. Nieuwenhuys and W.M.H. Sachtler, Surf. Sci. 34 (1973) 317.
[10] B.E. Nieuwenhuys, O.G. van Aardenne and W.M.H. Sachtler, Thin Solid Films 17 (1973) S7–S11.
[11] R. Bouwman and W.M.H. Sachtler, J. Catal. 19 (1970) 127.
[12] R. Bouwman and W.M.H. Sachtler, Surf. Sci. 24 (1971) 350.
[13] R. Bouwman, G.J.M. Lippits and W.M.H. Sachtler, J. Catal. 25 (1972) 350.
[14] R. Bouwman and W.N.H. Sachtler, J. Catal. 26 (1972) 63.
[15] W.M.H. Sachtler. Le Vide 163–165 (1973) 19.
[16] C. Dossi, J. Schaefer and W.M.H. Sachtler, J. Mol. Catal. 52 (1989) 193.
[17] N. Herron, G.D. Stucky and C.A. Tolman, Inorganica Chimica Acta 100 (1985) 135.
[18] L.L. Sheu, H. Knözinger and W.M.H. Sachtler, Catal. Lett. 2 (1989) 129.
[19] L.L. Sheu, H. Knözinger and W.M.H. Sachtler, J. Am. Chem. Soc. 111 (1989) 8125.
[20] L.L. Sheu, H. Knözinger and W.M.H. Sachtler, J. Mol. Catal. 57 (1989) 61.
[21] Z. Zhang, W.M.H. Sachtler and H. Chen, Zeolites 10 (1990) 784.
[22] S.T. Homeyer and W.M.H. Sachtler, J. Catal. 117 (1989) 91.
[23] G. Bergeret, P. Gallezot and B. Imelik, J. Chem. Phys., 85 (1981) 411.
[24] G. Bergeret and P. Gallezot, J. Chem. Phys. 87 (1983) 1160.
[25] P. Gallezot and B. Imelik, Adv. Chem. Ser. 121 (1973) 66.
[26] Z. Zhang, W.M.H. Sachtler. and H. Chen, Zeolites 10 (1990) 784.
[27] Z. Zhang, H. Chen and W.M.H. Sachtler, J. Chem. Soc., Faraday Trans., in press.
[28] S.T. Homeyer and W.M.H. Sachtler, J. Catal. 118 (1989) 266.
[29] S.T. Homeyer and W.M.H. Sachtler, J. Catal. 118 (1989) 266.
[30] Z. Zhang, H. Chen, L.L. Sheu and W.M.H. Sachtler, J. Catal., in press..
[31] Z. Zhang, T. Wong and W.M.H. Sachtler, J. Catal., in press.
[32] Z. Zhang, W.M.H. Sachtler and S. Suib, Catal. Lett. 2 (1989) 395.
[33] J.S. Feeley and W.M.H. Sachtler, Zeolites 10 (1990) 738.
[34] Z. Zhang and W.M.H. Sachtler, J. Chem. Soc., Faraday Trans. 86 (1990) 2313.
[35] Z. Zhang and W.M.H. Sachtler, J. Mol. Catal., in press.
[36] Z. Zhang and W.M.H. Sachtler, to be published.
[37] M.L. Poutsma, L.F. Elek, P.A. Ibarbia, A.P. Risch and J.A. Rabo, J. Catal. 52 (1978) 157.
[38] Y. Kikuzono, S. Kagami, S. Naito, T. Onishi and K. Tamaru, Faraday Disc., Chem. Soc. 72 (1981) 135.
[39] F. Fajula, R.G. Anthony and J.H. Lunsford, J. Catal. 73 (1982) 237.
[40] J.M. Driessen, E.K. Poels, J.P. Hindermann and V. Ponec, J. Catal. 82 (1983) 26.
[41] J.S. Rieck and A.T. Bell, J. Catal. 103 (1987) 46.
[42] F.A.P. Cavalcanti, C. Dossi, L.L. Sheu and W.M.H. Sachtler, Catal. Lett. 6 (1990) 289.
[43] T.M. Tri., J.P. Candy, P. Gallezot, J. Massardier, M. Primet, J.C. Védrine and B. Imelik, J. Catal., 79 (1983) 396.
[44] K. Foger and J.R. Anderson, J. Catal. 54 (1978) 318.
[45] A.Y. Stakheev and W.M.H. Sachtler, unpublished results.
[46] C. Besoukhanova, J. Guidot, D. Barthomeuf, M. Breysse and J.R. Bernard, J. Chem. Soc., Faraday I, 77 (1981) 1595.
[47] R.A. Dalla Betta and M. Boudart, in: *Proc. 5th Int. Congr. Catalysis*, ed. H. Hightower (North-Holland, Amsterdam, 1973) p. 1329.
[48] S.T. Homeyer, Z. Karpinski and W.M.H. Sachtler, J. Catal. 123 (1990) 60.

[49] S.T. Homeyer, Z. Karpiński and W.M.H. Sachtler, Recl. Trav. Chim. Pays-Bas (J. Roy. Neth. Chem. Soc.) 109 (1990) 81.
[50] D.M. Brouwer, in: *Chemistry and Chemical Engineering of Catalytic Processes*, eds. R. Prins and G.C.A. Schuit (Sijthoff and Noordhoff, Alphen a.d. Rijn, Netherlands and Germantown, Ml, USA, 1980) p. 137–160.
[51] X.L. Bai and W.M.H. Sachtler. J. Catal., in press.
[52] X. Bai and W.M.H. Sachtler, J. Catal., submitted.